Proc. Natl. Acad. Sci. USA
Vol. 87, pp. 6068–6072, August 1990
Medical Sciences

Listeria monocytogenes moves rapidly through the host-cell cytoplasm by inducing directional actin assembly

(actin polymerization/α actinin/tropomyosin/myosin/nonmuscle cells)

GUISSOU A. DABIRI*, JEAN M. SANGER†, DANIEL A. PORTNOY‡, AND FREDERICK S. SOUTHWICK*§

Departments of *Medicine, Infectious Disease Section, 536 Johnson Pavilion, and †Anatomy, and ‡Microbiology, University of Pennsylvania School of Medicine, Philadelphia, PA 19104

Communicated by Louis B. Flexner, May 8, 1990

ABSTRACT **_Listeria monocytogenes_ is an intracellular parasite that can readily infect the macrophage-like cell line J774 and the kidney epithelial cell PtK2. After being ingested, the organism escapes from the phagolysosome into the host-cell cytoplasm. *N*-(7-Nitrobenz-2-oxa-1,3-diazol-4-yl)-phallacidin, a specific stain for actin filaments (F-actin), demonstrates that within 1 hr of initiation of infection, the bacteria become surrounded by host-cell cytoplasmic actin filaments. By 3 hr, long projections of F-actin begin to form at one end of the bacteria. These actin structures colocalize with the actin-bundling protein α-actinin as well as with tropomyosin. Microinjection of fluorescently labeled α-actinin in living cells demonstrates that the formation of these F-actin projections is associated with bacterial movement, actin filaments rapidly assembling behind the bacteria as they migrate through the cytoplasm. These F-actin tails attain lengths up to 40 μm. The movement of the bacteria through the cytoplasm is rapid, 0.12–1.46 μm/sec. Within 2 min of cytochalasin D (0.5 μg/ml) treatment, all bacterial intracellular movement stops, and additional bacteria-associated actin assembly is blocked. A nonmotile *Listeria* mutant induces comparable actin assembly and moves at speeds similar to the wild type, indicating that the forces required for intracellular bacterial movement are generated by the host cell. *L. monocytogenes* can dramatically stimulate host-cell actin assembly in a directional manner, which serves to rapidly propel the bacteria through the cytoplasm, allowing the organisms to move to peripheral membranes and spread to uninfected cells.**

Listeria monocytogenes is an intracellular parasite that can cause serious, sometimes fatal infections in pregnant women, newborns, and immunocompromised patients. This Gram-positive rod-shaped bacterium has a similar intracellular life style to several other parasites, including *Shigella flexneri*, *Rickettsiae*, and *Trypansoma cruzi*. These organisms are all capable of growing and replicating directly within the host-cell cytoplasm (1).

Listeria are actively internalized by host cells and incorporated into phagolysosomes. The bacteria then escape from the phagolysosome and enter the cytoplasm (2–5). This process requires hemolysin because nonhemolytic mutants remain in the phagolysosome and consequently are avirulent in mice (2, 6–8). After escaping into the cytoplasm, the organism spreads from cell to cell (2) by moving to the peripheral membrane, where it induces the formation of filopodia-like cytoplasmic projections that are subsequently ingested by adjacent cells (4).

Recent evidence suggests that *L. monocytogenes* conscripts the contractile apparatus of the host cell to transport itself and spread from cell to cell. On escaping from the phagolysosome into the peripheral cytoplasm, *Listeria* becomes surrounded by cytoplasmic actin filaments (4, 9, 10). At later times actin filaments are seen at one end of the bacterium, where they extend outward, forming a single long projection (4). Cytochalasin D treatment of host cells prevents the formation of these actin projections and blocks bacterial cell-to-cell spread, indicating that host-cell actin filament assembly plays an important role in intracellular *Listeria* motility (4).

A number of questions have been raised by these findings. Are other contractile proteins present in these actin-based structures? How rapidly do the bacteria move within the cell and how quickly are the long projections of F-actin formed? Are these projections truly tails—i.e., are they seen on the side opposite to the direction of bacterial movement? Does actin assembly provide the propulsive force for bacterial movement?

Using fluorescent microscopy of fixed and living J774 and PtK2 cells, we have addressed these issues. Most surprising is our finding that *Listeria* can move within the host cytoplasm at very rapid speeds (to 1.46 μm/sec), leaving behind long trails of actin filaments that can extend nearly the full length of the host cell.

MATERIALS AND METHODS

Bacterial Strains and Growth Conditions. Four strains were used in this study. 10403S is a virulent strain (11) that belongs to serotype 1, is resistant to streptomycin at 1 mg/ml, and has an LD_{50} for mice of 3×10^4. Strain DPL-881 is a Tn*916* mutant of 10403S. This virulent strain fails to migrate on soft agar plates or exhibit motility when observed under phase microscopy (D.A.P., unpublished data). Strain DPL-910 is a virulent 10403S strain harboring the plasmid pLTV3 encoding chloramphenicol resistance (A. Camilli and D.A.P., unpublished data). Strain DPL-215 is an avirulent nonhemolytic mutant of strain 10403S with an LD_{50} of $>10^9$ (7).

Tissue Culture Cells and Growth Medium. The macrophage-like cell line J774 (12) was obtained from J. Unkeless (Mount Sinai Medical School, New York) and grown as described (7). PtK2 cells, derived from rat kangaroo kidney epithelial cells, were obtained from American Type Culture Collection and were grown on glass coverslips as described (13).

Infection. An inoculum of 1×10^6 *L. monocytogenes* per ml was used to infect J774 cell monolayers (7). PtK2 cells were infected with a higher innoculum of organisms, 1×10^7/ml. As has been described (2, 7), gentamicin sulfate was added to the medium 60 min after initiation of infection to prevent extracellular growth of organisms.

Fluorescence Labeling of F-Actin, α-Actinin, Tropomyosin, and Bacteria. Cells were fixed with 3.7% (vol/vol) formaldehyde in phosphate-buffered saline for 15 min or more at

The publication costs of this article were defrayed in part by page charge payment. This article must therefore be hereby marked "*advertisement*" in accordance with 18 U.S.C. §1734 solely to indicate this fact.

Abbreviations: NBD-phallacidin, *N*-(7-nitrobenz-2-oxa-1,3-diazol-4-yl)-phallacidin; LR, lissamine rhodamine sulfonyl chloride.

§To whom reprint requests should be addressed.

25°C followed by treatment with 0.4% Triton X-100 and 1.7 × 10^{-7} M *N*-(7-nitrobenz-2-oxa-1,3-diazol-4-yl)-phallacidin (NBD-phallacidin) (Molecular Probes) for 10 min at 37°C (14). Intracellular bacteria were stained as described (7) by using *Listeria* O rabbit antiserum. In several experiments F-actin was stained with 1.7 × 10^{-7} M rhodamine–phalloidin (Molecular Probes), and the bacteria were stained with a 1:40 dilution of fluorescein isothiocyanate-conjugated goat F(ab')2 anti-rabbit IgG (Tago).

α-Actinin or tropomyosin were localized by immunofluorescence as described (15). The anti-α-actinin and antitropomyosin antibodies were both obtained from Sigma.

Microinjection of Labeled Proteins. Before infection with bacteria, cells were microinjected with lissamine rhodamine sulfonyl chloride (LR)-labeled α-actinin, myosin light chain, or bovine serum albumin by using a pressure-injection system as described (13).

Cytochalasin D Treatment. For NBD-phallacidin studies, cells were exposed to medium containing Dulbecco's modified Eagle's medium with gentamicin at 5 μg/ml and cytochalasin D at 0.5 μg/ml. For live observations, coverslips were mounted with a partial seal of vaseline to allow medium to be perfused through the cell preparation. Five volumes of medium containing cytochalasin D (0.5 μg/ml) were perfused through the coverslip chamber, and a similar volume of control medium was later perfused through to remove the cytochalasin.

Microscopy and Image Processing. Cells were observed with epifluorescence on an Olympus Vanox photomicroscope using a silicon intensified target camera (Dage-MIT, Michigan City, IN) coupled to an image-processing system (Image-I/AT, Media, PA). Images were subjected to frame summation and then photographed with a 35-mm camera from the video monitor.

RESULTS

NBD-Phallacidin Staining of Infected Cells at Various Times After Infection. Within 60 min of exposure to bacteria (Figs. 1 and 2), ≈40% of the bacteria were surrounded by F-actin. By 90 min the number of bacteria surrounded by F-actin had increased to 80%, and by 240 min all the bacteria colocalized with F-actin. After infection with the mutant hemolysin-negative strain, no F-actin was seen after 240 min of infection (data not shown). Because the nonhemolytic mutant remains in the phagolysosome, this finding suggested that only cytoplasmic *L. monocytogenes* become associated with F-actin.

In addition to colocalizing with discrete NBD-phallacidin staining, at 240 min, 11.6 ± 2.0% (mean ± SEM; n = 22 microscopic fields) of the wild-type bacteria demonstrated projections of NBD-phallacidin stain extending from one end of the bacteria (Fig. 2). The length of these projections varied greatly—some were as long as 30 μm. The presence of these projections was first observed after 3 hr. When cells were treated with chloramphenicol (20 μg/ml) 1 hr after initiating infection and then observed at 4 hr, no bacteria-associated actin assembly was seen. If chloramphenicol treatment was delayed for 2 hr after initiating infection, cells frequently contained bacteria surrounded by F-actin as well as bacteria containing F-actin projections; however, at 4 hr not all bacteria colocalized with F-actin as seen in control cells (data not shown). Chloramphenicol treatment of cells infected with a chloramphenicol-resistant mutant demonstrated the same F-actin morphologies as untreated cells infected with the wild-type *Listeria* strain.

Microinjection of Living Cells with Fluorescently Labeled Contractile Proteins. The nature of the F-actin projections was clarified by microinjecting living J774 and PtK2 cells with trace amounts of a rhodamine-labeled actin-binding protein, α-actinin-LR, before infection. Video images of live microinjected cells demonstrated that as the bacteria moved they left behind a trail of F-actin (Fig. 3). Microinjection of fluorescently labeled bovine serum albumin, BSA-LR, failed to localize around the bacteria and did not result in tails (data not shown).

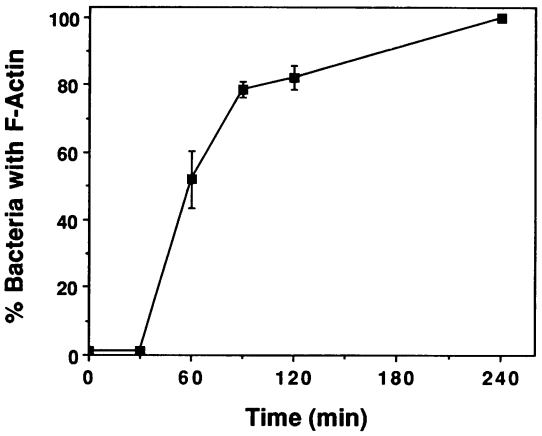

FIG. 1. Time course of filamentous actin formation after *L. monocytogenes* infection of J774 cells. The macrophage-like J774 cells were infected with *L. monocytogenes* at time 0 min as described. At indicated times cells were fixed, permeabilized, and stained with NBD-phallacidin. Cells were then incubated with *Listeria* O rabbit antisera followed by a rhodamine-labeled secondary antibody. Fluorescence photomicrographs at 510- and 575-nm emission wavelengths were compared, and the percentages of bacteria in which the two stains colocalized were determined over time. Samples represent the mean of three separate experiments; bars represent SEM. Total numbers of bacteria analyzed for each time point were as follows: 30 min, 87; 60 min, 141; 90 min, 99; 120 min, 198; 240 min, 699.

Intracellular bacterial movement within live cells was rapid. Fig. 3 represents sequential images of one bacterium that moved 50 μm in 85 sec and a second bacterium in the same cell that traveled 29 μm in 54 sec. The mean speed(± SEM) of bacterial movement in J774 cells (0.60 ± 0.04 μm/sec; n = 31) was significantly faster than in PtK2 cells (0.22 ± 0.004 μm/sec; n = 76, $P < 0.001$, unpaired Student's t test). Unlike J774, PtK2 cells have an extensive network of stress fibers. These fibers appeared to be unaltered for at least the first 6 hr after infection. Observations of single bacteria also revealed that the speed of migration varied considerably from time point to time point in each cell type, ranging from 0.25 to 1.46 μm/sec in J774 cells and from 0.12 to 0.35 μm/sec in PtK2 cells (see Fig. 6). Time-lapse videos of bacterial movement clearly demonstrated that the bacteria did not pull the tails along as they moved; rather the F-actin tails remained stationary in the cytoplasm—bacterial move-

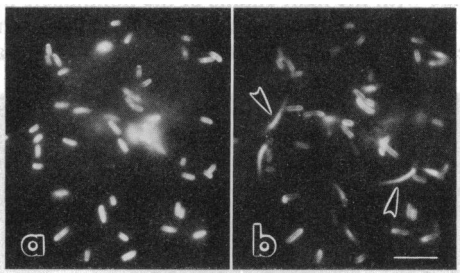

FIG. 2. Fluorescence micrographs of hemolysin$^+$ *Listeria*-infected J774 cells stained with both antibacterial antibody and NBD-phallacidin. (*a*) Rhodamine fluorescent antibacterial antibody stain. (*b*) NBD-phallacidin stain. In *b*, in addition to phallacidin localization around the bacteria, projections of F-actin were found associated with some bacteria (see arrowheads). Cells were infected, fixed, and stained as described for Fig. 1. (Bar = 10 μm.)

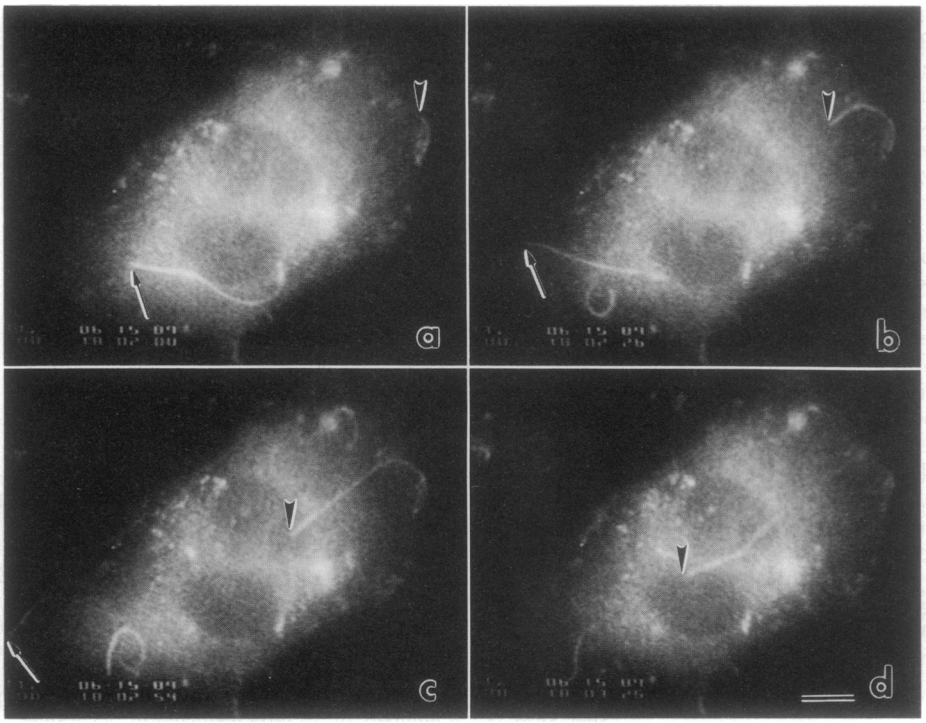

FIG. 3. Fluorescence photomicrographs of live J774 cells microinjected with fluorescently labeled α-actinin. Cells were microinjected with LR-labeled α-actinin 1 hr before infection with *L. monocytogenes*. Sequential micrographs were taken 4 hr after infection. Times required to migrate from point a to b, c, and d were 26, 54, and 85 sec, respectively. The arrows point to a bacterium migrating toward the peripheral membrane at 0.54 μm/sec; arrowheads point to a second bacterium moving at 0.63 μm/sec. In the left lower corner of *b* and *c*, a third bacterium can be seen circling within the cytoplasm. (Bar = 10 μm.)

ment being associated with progressive actin filament assembly near the bacteria and rapid lengthening of the tails.

As suggested by our fixed preparations, living cells failed to demonstrate bacterial movement and tail formation until 3 hr after addition of bacteria to the cell preparations. By 3.5 hr bacteria were seen moving rapidly within the cytoplasm, leaving long tails of fluorescence behind them. In some cases bacteria moved in a circular pattern. In one instance, after circling within the cytoplasm, the bacteria moved out toward the peripheral membrane, pushing outward to form a long narrow projection containing the bacteria in the distal portion. In other instances bacteria were seen to move in a nearly straight line, leaving long tails of F-actin (to 40 μm), and then to stop on reaching the peripheral cell membrane.

Although bacterial movement within cells was rapid, it was only a fraction of the rate seen in extracellular bacteria (10 μm/sec); therefore, to eliminate the possibility that the inherent motile system of the bacterium was responsible for the observed intracellular movement, we infected PtK2 cells with a nonmotile *Listeria* mutant. Intracellular migration speeds (0.22 ± 0.01 μm/sec, n = 31) and F-actin tail formation were identical with the wild-type strain.

In addition to labeled α-actinin, cells were injected with myosin light chain-LR. These light chains would be expected to exchange with the light chains of the nonmuscle myosin II (13). Even when injected 24 hr before infection to maximize exchange of fluorescent and native protein, no colocalization with the bacteria was seen. This protein also failed to concentrate in the filamentous actin tails seen later in the infection.

Anti-α-Actinin and Antitropomyosin Antibody Staining of Fixed Cells. As shown in Fig. 4, the actin filament crosslinking protein, α-actinin, was highly enriched in the areas containing F-actin. Localization of F-actin and α-actinin were examined simultaneously by also staining the preparations with NBD-phallacidin. In bacteria containing tails, F-actin was enriched at the back end and tail region of the bacteria, but not at the head region, whereas α-actinin uniformly surrounded the bacteria as well as localizing in the actin filament tail (Fig. 4 *b* and *c*). Cells were also stained by using antitropomyosin antibody. The pattern of staining was similar to α-actinin.

Effects of Cytochalasin D. Coverslips containing adherent cells were exposed to cytochalasin D either before infection or after 60 min of infection. After 4 hr, cytochalasin-treated cells demonstrated only very small punctate regions of staining near some of the bacteria, and F-actin tails were absent (Fig. 5). Because uninfected cytochalasin D-treated cells failed to demonstrate punctate staining, this staining pattern was induced by bacteria. Identical results were seen whether cytochalasin D was added before or after initiation of infection. Use of rhodamine-labeled phallacidin and a fluorescein bacterial stain resulted in an identical staining pattern.

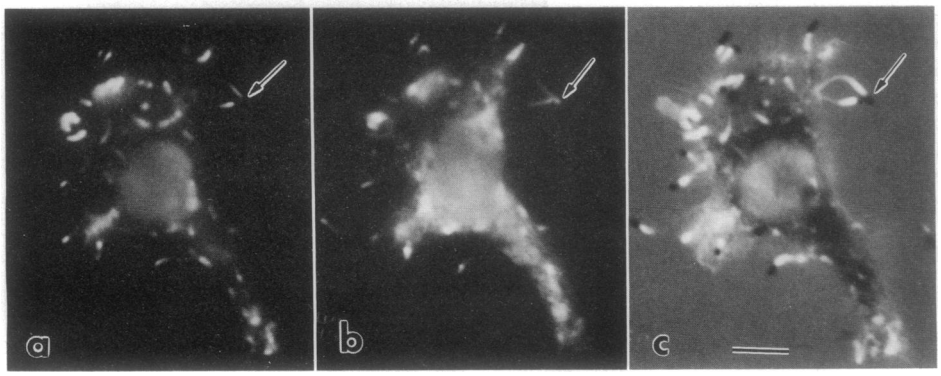

FIG. 4. Fluorescence photomicrographs of infected J774 cells stained with both anti-α-actinin antibody and NBD-phallacidin. (*a*) NBD-phallacidin stain. (*b*) Anti-α-actinin stain. (*c*) Computer-generated image in which the anti-α-actinin image (*b*) was subtracted from the phallacidin image (*a*), and the result was enhanced to emphasize differences in the two images. The black in *c* shows α-actinin present around many of the bacteria to a greater extent than phallacidin. Arrows point to one example. (Bar = 10 μm.)

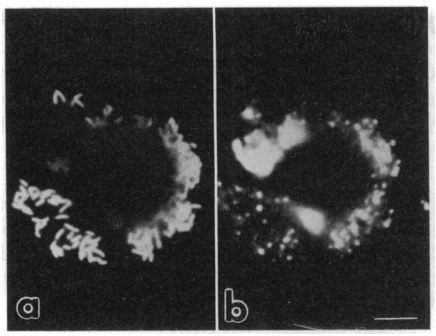

FIG. 5. Fluorescence photomicrographs of infected J774 cells treated with cytochalasin D before staining with NBD-phallacidin. (*a*) Anti-bacterial antibody stain. (*b*) NBD-phallacidin stain. Cells were prepared as described for Fig. 1, with the exception that after 60 min of infection, coverslips were transferred to medium containing cytochalasin D at 0.5 μg/ml. Cells were viewed at 4 hr. (Bar = 10 μm.)

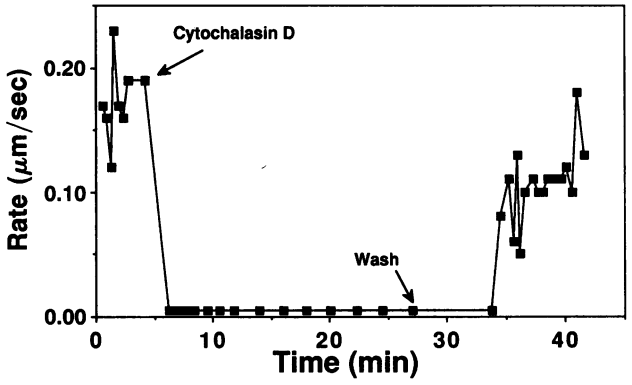

FIG. 6. The speed of *L. monocytogenes* intracellular migration in PtK2 cells before, during, and after cytochalasin D treatment. PtK2 cells were microinjected with LR-labeled α-actinin 1 hr before infection. By 4 hr after infection bacteria were actively migrating in the cytoplasm. Serial images of a single moving bacteria were saved on the image analyzer. At the times depicted, the distance migrated during a short interval (30 sec) was measured. After 4-min observation the cells were perfused with 5 vol of medium containing cytochalasin D at 0.5 μg/ml. Within 2 min, the earliest observation time, the bacteria had completely stopped moving. No additional bacteria-associated actin filament assembly was seen. After 22 min the cytochalasin was washed out by perfusing the cells with 5 vol of medium. Within ≈7 min the bacteria began to extend actin filaments from the bacterial side of the tail. Actin assembly was again associated with movement of the bacteria.

Addition of cytochalasin D to live microinjected PtK2 cells infected for 4 hr resulted in the abrupt (within 2 min) inhibition of all bacterial movement (Fig. 6) and newly formed bacteria-associated actin assembly. Removal of cytochalasin D resulted in partial recovery of movement and tail formation by 7 min. During the 22 min cells were exposed to cytochalasin D, the tails did not totally disappear; however, fluorescence became less intense. On removal of this agent new actin filament growth was associated with brighter fluorescence (data not shown). This new growth appeared on the bacterial ends of the actin tails. For the period after cytochalasin D treatment (14.5 min), speeds of migration were significantly slower than pretreatment speeds (0.11 ± 0.01 μm/sec, $n = 14$ vs. 0.17 ± 0.01 μm/sec, $n = 8$, $P < 0.001$).

DISCUSSION

The growth of *L. monocytogenes* in cultured cells provides a useful model for understanding how an intracytoplasmic parasite regulates actin assembly. This model is of interest not only to the microbiologist but also to investigators of contractile protein biochemistry because the mechanisms that induce actin assembly during this infection probably bypass the usual signal-transduction pathways associated with membrane receptor-mediated actin polymerization.

To better characterize the time course of these reactions, we first used NBD-phallacidin staining and fluorescence microscopy. This method allowed analysis of hundreds of bacteria in infected cells as compared with previous EM studies that sampled only small numbers of organisms (4). Two distinct morphologies of F-actin were seen. Early in the experiments, within 60 min of initiating infection, almost half of the bacteria were surrounded by F-actin, and by 90 min almost all bacteria colocalized with filamentous actin. Because electron micrographs have shown that bacteria begin to escape from the phagolysosome after 30 min of infection (4), we conclude that actin filaments formed around the bacteria within 30–60 min of the bacteria entering the cytoplasm. More detailed resolution of the time course was not possible because true synchronous entry of bacteria into the cytoplasm could not be readily achieved. Treatment with chloramphenicol, an antibiotic that prevents bacterial replication and inhibits bacterial protein synthesis, blocked bacteria-associated actin assembly, suggesting that *de novo* bacterial protein synthesis may be required to start this process.

The second F-actin morphology was not seen until 3 hr after initiating infection when long projections of filamentous actin began to form within the host-cell cytoplasm. At the time points examined these projections were present on a minority of bacteria (≈11%). Often the projections extended beyond one focal plane, making it necessary to scan in several planes to accurately determine the number of bacteria associated with projections. This type of examination also revealed that a minority of bacteria contained projections. For a projection to be detected by fluorescence microscopy, however, NBD-phallacidin staining had to clearly extend beyond the bacterial antibody fluorescence image. Short projections of <1 μm would not have been detected. Therefore, our methods may underestimate the exact percentage of bacteria with actin projections. Treatment with chloramphenicol 2 hr after infection, when actin filaments had surrounded the bacteria, failed to inhibit formation of actin projections, suggesting that this transition in actin architecture does not require active bacterial protein synthesis or bacterial cell division.

The nature of these actin filament projections was clarified in two ways: (*i*) by immunofluorescence and (*ii*) by microinjection of living cells with fluorescently labeled α-actinin. Microinjection of live cells demonstrated that the long projections of actin always formed in the direction opposite to that of bacterial movement, the bacteria leaving trails of F-actin as they moved. Several types of movement were seen. Most bacteria moved in a circular pattern; less commonly they moved in a straight line. In several instances, on reaching the peripheral membrane the bacteria continued to move outward forming a long narrow filapodia-like structure. At any one time a minority of the bacteria were noted to be moving. The rate of movement also varied. Speeds of up to 1.46 μm/sec were noted in J774-infected cells, whereas the maximal rate of migration in PtK2 cells was 0.35 μm/sec. This difference in speed may be due to the extensive network of actin stress fibers, intermediate filaments, and microtubules present in PtK2 cells, which could impede bacterial movement through the cytoplasm. Alternatively, PtK2 cells may contain less monomeric actin available for filament assembly.

The fluorescent images seen in microinjected cells was assumed to be due to exchange of the fluorescent analogue of α-actinin with the endogenous α-actinin in the actin micro-

filaments as occurs in stress fibers, cleavage furrows, and other structures in the cell (13). Anti-α-actinin antibody concentrated in this same location, confirming this assumption. Polymerization of actin in the presence of α-actinin, which is known to crosslink actin filaments (16, 17), may explain the complex network of short actin filaments seen in electron micrographs (4). It is also possible that α-actinin may serve to enhance actin filament assembly by serving as a nucleus for filament elongation (18). Tropomyosin also colocalized with the bacteria-associated F-actin and may serve to protect filaments from cleavage by severing proteins such as gelsolin (24), known to be present in the cytoplasm of nonmuscle cells.

Does host-cell actin filament assembly generate the forces responsible for rapid intracellular bacterial movement? All our findings are consistent with this conclusion. Experiments with a nonmotile *Listeria* mutant prove that the normal motile machinery of this bacteria is not required for intracellular movement and support the conclusion that the host must generate the forces required for bacterial motility in the cytoplasm. Time-lapse video microscopy of living cells indicates that the F-actin tails are not dragged along with the bacteria but rather appear to be anchored within the cytoplasm. Tails increase in length as the bacteria continue to migrate, filament elongation taking place in close proximity to the bacteria. Cytochalasin D, an agent that blocks actin filament growth at the barbed or fast-growing end of actin filaments, rapidly blocks elongation at the bacterial end of the F-actin tails and is associated with complete inhibition of bacterial movement. These observations are all consistent with the conclusion that barbed-end host-cell actin filament growth provides the force for movement of the bacteria through the cytoplasm.

Previous electron micrographs of myosin S1-labeled F-actin tails also support this conclusion. Careful review of these micrographs reveals that all the actin filaments were oriented with the barbed, or fast growing, ends facing toward the bacteria (4). This orientation of actin filaments, as well as the failure of myosin light chains to localize in the tails, makes myosin II an unlikely candidate for generating the forces required for intracellular bacterial movement. However, myosin I remains a possible component of this intracellular motor. Myosins can produce movements of 1 μm/sec in *in vitro* systems (19); however, actin filament elongation could also produce movements at this rate. Were 40 μM monomeric actin available for assembly, a calculated elongation rate of 1 μm/sec could be achieved. Nonmuscle cells contain ≈200 μM monomeric actin. Therefore, *L. monocytogenes* would be required to stimulate the release of approximately one-fifth of the total unpolymerized actin pool to propel itself through the cytoplasm of the host cell.

Recent reports suggest that *S. flexneri*, another intracellular pathogen, can interact with the host-cell microfilaments (20). This Gram-negative parasite penetrates epithelial cells, grows in the cytoplasm, and spreads from cell to cell similarly to *L. monocytogenes* (20, 21). A 120- to 140-kDa outer-membrane protein has been identified in *S. flexneri* that may be involved in the interaction of the bacterial surface with cytoplasmic contractile proteins (20, 22, 23). It will be important to look for similar proteins in *Listeria*.

We thank Dr. Annemarie Weber for her calculations of actin-filament assembly rates. This work was supported by National Institutes of Health Grants 5T32-HL07502 (G.A.D.), HL15,835 (to the Pennsylvania Muscle Institute, J.M.S.), AI27655 (D.A.P.), and AI 123262 (F.S.S.).

1. Moulder, J. W. (1985) *Microbiol. Rev.* **49,** 298–337.
2. Havel, E. (1986) *Infect. Immun.* **54,** 787–792.
3. Racz, P., Tenner, K. & Mero, E. (1972) *Lab. Invest.* **26,** 1694–1700.
4. Tilney, L. G. & Portnoy, D. A. (1989) *J. Cell Biol.* **109,** 1597–1608.
5. Gaillard, J.-L., Berche, P., Mounier, J., Richard, S. & Sansonetti, P. (1987) *Infect. Immun.* **55,** 2822–2829.
6. Gaillard, J.-L., Berche, P. & Sansonetti, P. (1986) *Infect. Immun.* **52,** 50–55.
7. Portnoy, D. A., Jacks, P. S. & Hinrichs, D. J. (1988) *J. Exp. Med.* **167,** 1459–1471.
8. Kuhn, M., Kathariou, S. & Goebel, W. (1988) *Infect. Immun.* **56,** 79–82.
9. Southwick, F. S., Dabiri, G. A. & Portnoy, D. A. (1989) *Clin. Res.* **37,** 567 (abstr.).
10. Mounier, J., Ryter, A., Coquis-Rondon, M. & Sansonetti, P. J. (1990) *Infect. Immun.* **58,** 1048–1058.
11. Bishop, D. K. & Hinrichs, D. J. (1987) *J. Immunol.* **139,** 2005.
12. Ralph, P. & Prichard, J. (1975) *J. Immunol.* **114,** 898.
13. Mittal, B., Sanger, J. M. & Sanger, J. W. (1987) *J. Cell Biol.* **105,** 1753–1760.
14. Howard, T. H. & Oresajo, C. O. (1985) *J. Cell Biol.* **101,** 1078–1085.
15. Sanger, J. W., Sanger, J. M. & Jockusch, B. M. (1983) *J. Cell Biol.* **96,** 961–969.
16. Podlubnaya, X. A., Tskhovrebova, L. A., Zaalishvili, M. M. & Stefanenko, G. A. (1975) *J. Mol. Biol.* **92,** 357–359.
17. Bennett, J. P., Zaner, K. S. & Stossel, T. P. (1984) *Biochemistry* **23,** 5081–5086.
18. Blikstad, I., Eriksson, S. & Carlson, L. (1980) *Eur. J. Biochem.* **109,** 317–323.
19. Warrick, H. M. & Spudich, J. A. (1987) *Annu. Rev. Cell Biol.* **3,** 379–421.
20. Bernardini, M. L., Mounier, J., D'Hauteville, H. D., Coquis-Rondon, M. & Sansonetti, P. J. (1989) *Proc. Natl. Acad. Sci. USA* **86,** 3867–3871.
21. Sansonetti, P. J., Ryter, A., Clerc, P., Maurelli, A. T. & Mounier, J. (1986) *Infect. Immun.* **51,** 461–469.
22. Pal, T., Newland, J. W., Tall, B. D., Formal, S. B. & Hale, T. T. (1990) *Infect. Immun.* **57,** 477–486.
23. Lett, M.-C., Sasakawa, C., Okada, N., Sakai, T., Makino, S., Yamada, M., Komatsu, K. & Yoshikawa, M. (1990) *J. Bacteriol.* **171,** 353–359.
24. Fattoum, A., Hartwig, J. H. & Stossel, T. P. (1983) *Biochemistry* **22,** 1187–1193.